Calculation of the Stopping-Muon Rate Underground*

G. L. Cassiday, J. W. Keuffel, and J. A. Thompson†
Department of Physics, University of Utah, Salt Lake City, Utah 84112
(Received 17 July 1972)

A detailed calculation is given for the rate of stopping cosmic-ray muons underground. An important source of such muons, dominant at depths $\gtrsim 1.5\times10^5$ g/cm^2, is the decay of slow pions which are the end products of hadronic cascades in the rock initiated by the photonuclear interactions of fast muons. The cross section for the production of such cascades is obtained by extrapolating accelerator data to higher energies. The multiplicity of stopping pions is taken from a detailed Monte Carlo calculation. The results agree with the observed rates of stopping muons and of identified stopping pions at shallow depths. An explanation is offered for the Turin measurements of stopping muons made at shallow depths and various inclined zenith angles. However, for the Turin point at 4.27×10^5 g/cm^2 (which is uniquely sensitive to a possible anomalous source of stopping muons) the predictions fall short by a factor of 4, and we are unable to account for the discrepancy even under the most extreme assumptions for the conventional processes considered.

I. INTRODUCTION

Much interest has been generated by the Turin observations[1-3] of a rate of stopping muons underground greatly in excess of the rate expected from the slope of the intensity vs depth curve of muons originating in the atmosphere. There has been some speculation that the excess stopping-muon rate might be a manifestation of new high-energy leptonic processes. A number of papers have since appeared[4-7] which seek to explain the excess muons as the decay products of locally produced pions. The calculations do not all agree, and the interpretations of the effect differ in some respects from one author to another.

In this paper, we present a detailed calculation of stopping-muon rates from the following sources: (1) atmospheric muons coming to the end of their range, (2) muons from the decay of slow pions generated locally by interactions of fast muons. The local pion production is calculated using extrapolations of accelerator data on inelastic muon scattering data and a detailed Monte Carlo calculation of the stopping-pion multiplicity in hadronic cascades. We do not consider muons induced by neutrinos (which are negligible for depths up to and including the deepest Turin point, as demonstrated by Grupen *et al.*[5]).

The stopping atmospheric muons are expected to have approximately the same angular distribution as the through-going muons. However, the locally produced muons are nearly isotropic (see Sec. III). The approach used in this paper is to calculate the intensity of stopping particles per g, regardless of incident direction. The intensity of locally produced particles is derived from the calculated production rates and slow-pion multiplicities via an equilibrium argument.

It is customary to quote results in terms of the ratio R of stopping muons to through muons. To avoid ambiguities due to differences in the angular distributions of the various stopping particles and of the through muons, the ratio R quoted by us is for an omnidirectional detector under a flat earth.

The ratio R is not independent of detector size: the rate of muons stopping in a detector is proportional to the detector mass M, while the rate of muons passing through the detector is proportional to the area A presented in a given direction. The ratio R is thus proportional to the effective thickness M/A. In this paper, the calculations of R will refer to a spherical detector of effective thickness 100 g/cm^2 of standard rock ($Z=11$, $A=22$), and all experimental results will be normalized to such a detector.[8] The absolute intensity of stopping particles per g will also be given.

It should be noted that most detectors used to measure stopping underground particles have included coincidence or anticoincidence counters. The angular acceptances of these arrays, as well as their response to complex hadronic cascades, can in some cases dramatically affect the observed R values. Such effects are taken into account in Sec. VI when we compare existing experiments with our calculations.

II. STOPPING ATMOSPHERIC MUONS

The ratio, $R_a(h)$, of stopping atmospheric muons to penetrating muons has been calculated from the muon intensity-depth curve by many authors.[4-7,9] There is general agreement on $R_a(h)$ for the verti-

cal case. We extend the calculations to the case of an isotropically active detector open to muons incident from all directions, using the flat earth approximation. The slant depth h at zenith angle θ is then $h(\theta) = h_0 \sec\theta$, where h_0 is the vertical depth.

Letting $I(h, \theta)$ denote the integral muon intensity, the ratio of muons stopping in a detector of effective thickness $\Delta x(\theta, \varphi)$ and a projected area $A(\theta, \varphi)$ in the direction θ, φ is

$$S_a(h) = \int_\Omega \frac{dI(h+x, \theta)}{dx} \Delta x(\theta, \varphi) A(\theta, \varphi) d\Omega$$
$$= M \int \frac{dI}{dx} d\Omega, \quad (1)$$

where the detector mass $M = \Delta x A$ regardless of the orientation.

The through-going muon intensity is

$$N(h) = \int_\Omega I(h, \theta) A(\theta, \varphi) d\Omega$$
$$= \bar{A} \int I d\Omega$$
$$= \bar{A} I_V \Omega^* \quad (2)$$

and

$$R_a(h) = S_a(h)/N(h). \quad (3)$$

We note again that R_a is proportional to the effective detector thickness $\bar{t} = M/\bar{A}$, which for a spherical detector of radius r (in g/cm^2) is $\frac{4}{3}r$.

To evaluate $I(h, \theta)$ we express it as

$$I(h, \theta) = I_V(h) G(h, \theta), \quad (4)$$

where $I_V(h)$ is the vertical intensity-depth curve and $G(h, \theta)$ is the conventional atmospheric muon enhancement. For $I_V(h)$ at shallow depths (0–1000 hg/cm^2), we have used the fit of Stockel[10] to a function originally proposed by Miyake[11]

$$I_V(h) = A_0 \frac{h^{-\alpha}}{h + h_1} e^{-\beta h} \text{ sec}^{-1}\text{cm}^{-2}\text{sr}^{-1}, \quad (5)$$

with $A_0 = 45$, $\alpha = 1.38$, $h_1 = 162.5$, $\beta = 7.05 \times 10^{-4}$ and depths in units of hg cm^{-2} (1 hg cm^{-2} = 100 g cm^{-2}). For the deep depths (1000–10 000 hg/cm^2) we have used the fit by Groom[12]

$$I_V(h) = I_1 \exp(-h/\lambda_1) + I_2 \exp(-h/\lambda_2) \text{ sec}^{-1}\text{cm}^{-2}\text{sr}^{-1}, \quad (6)$$

where $I_1 = 12.8 \times 10^{-6}$, $I_2 = 1.13 \times 10^{-6}$, $\lambda_1 = 0.366 \times 10^3$ and $\lambda_2 = 0.794 \times 10^3$, and again depths are in units of hg cm^{-2}. $G(h, \theta)$ for the shallow depths is taken from Barrett *et al.*[13] and the effects of muon decay are included. We have also modified the results to include a small admixture of kaons. For $h < 500$ hg cm^{-2}, $G(h, \theta)$ is nearly one. For the deep depths we have used the results of Morrison[14] and here $G(h, \theta)$ is nearly $\sec\theta$; for these depths R_a is sensitive only to h. For the present, we have not considered the deviations from the $\sec\theta$ law indicated by the Utah experiment.[15] At depths where the Utah effect is appreciable, the muon intensity falls off very rapidly with zenith angle.

The results for R_a are shown in Fig. 4 (see Sec. VI). Also shown are the values of R_a obtained for vertical muons. One can see that even for atmospheric muons the stopping ratio can vary by a factor of 50% at shallow depths if a vertical trigger is used instead of an isotropically active detector.

III. STOPPING-PION MULTIPLICITIES IN HADRONIC CASCADES

The second important source of stopping muons underground is the decay of pions which have been produced locally as a result of the photonuclear interactions of through-going muons. A single such interaction may produce many stopping pions as the end products of a hadronic cascade. The multiplicity of stopping pions, $m(\nu)$, to be expected from a hadronic cascade of energy transfer ν is a crucial factor in determining the number of stopping muons to be expected from local muon interactions.

Since, at the time we began our work, there were neither measurements nor calculations of $m(\nu)$, a collaborative effort to calculate $m(\nu)$ was undertaken by one of us (J.A.T.) together with Jones and Johnson of Louisiana State University. The primary results of this paper[16] (hereinafter referred to as JJT) are reproduced in Fig. 1. The fit actually used by us was a polynomial in $\ln E$, rather than the line $m(\nu) = 0.8E^{0.75}$ shown in the figure, but the differences are negligible.

The sensitivity of $m(\nu)$ to different input assumptions was tested extensively, and a wide range of models with various single-collision multiplicities and momentum distributions all gave the same $m(\nu)$ to within 10% for momentum transfers up to a few hundred GeV. Since the inelastically produced particles carry only 40–50% of the incident energy in a single collision, the results for $m(\nu)$ do seem to be sensitive to the fraction of leading particles (scattered incident particles) which are charged. A prescription consistent with ionization spectrometer work (Model II) has been used, but also shown in Fig. 1 are the results from a diffraction model (Model I: 100% leading particles charged) and a quark model (Model III: 50% charged). It is seen, for example, that the multiplicities of Model I exceed those of Model II by a factor 1.7 at energy transfers $\gtrsim 100$ GeV. Existing analyses of accelerator data do not conclusively

resolve the leading charged particle question, presumably because of the difficulties of measuring neutrals and high-energy particles generally.

Strictly speaking, the JJT calculation is valid only for cascades initiated by pions. However, the same two limits of one and $\frac{1}{2}$ leading charged particles also seem reasonable for the photon (ρ^0); and $m(\nu)$ depends primarily upon the kinetic energy of the particle, rather than upon details of its interactions. Below 1 GeV, $m(\nu)$ has been calculated from known photon cross sections, assuming that all produced pions stop without interacting.

Because of the multiplicative nature of the cascade process, a change in the treatment of the low-energy interactions could shift $m(\nu)$ by nearly a constant scale factor for all energy transfers ν. Although the calculation of JJT treats the low-energy region carefully, one would like an experimental measurement of $m(\nu)$ to check the calculation. There are no such direct measurements of $m(\nu)$, but the stopping-pion rates measured at shallow depths are an indirect measure of $m(\nu)$ for the low-energy transfers ν important at these shallow depths. The agreement of these shallow depth measurements with our calculations (see Sec. VI C and Fig. 3) support our values of $m(\nu)$.

Angular distributions for the stopping muons are also given by JJT, who find that one-fourth of the stopping muons are going into the backward hemisphere, with respect to the shower axis, at the time they stop. Angular distributions are much more sensitive to the nuclear physics details than are the stopping-pion multiplicities. However, it seems clear that the distribution has in any case a strong contribution at ~90°. This fact, and the fairly broad spread in zenith angles of the high-energy muons, argue that the locally produced particles will be quasi-isotropic.

IV. STOPPING MUONS FROM MUON INELASTIC SCATTERING

A. Formulation of the Problem

The calculation of the rate of stopping muons generated by through-going ones is greatly facilitated by an equilibrium argument. The number of muons stopping in an underground detector is the same as the total number produced by interactions occurring in the detector regarded as a target. This argument is valid if the attenuation length of the through-going muons is much greater than the range of the generated secondaries.

The rate of stopping muons (which give rise to the 2.2 μsec signature used in most of the experiments) will then equal the rate of stopping pions, multiplied by the fraction η of pions which decay into muons. In condensed matter, essentially all the π^- undergo nuclear absorption, so that (assuming equal numbers of π^+ and π^-) $\eta = 0.5$. However, if the detector is located in a cavern, a fraction (typically 40%) of the π^- decay in flight to produce μ^-, which then mostly decay to give a 2.2 μsec signature. Numerical results are quoted using $\eta = 0.7$.

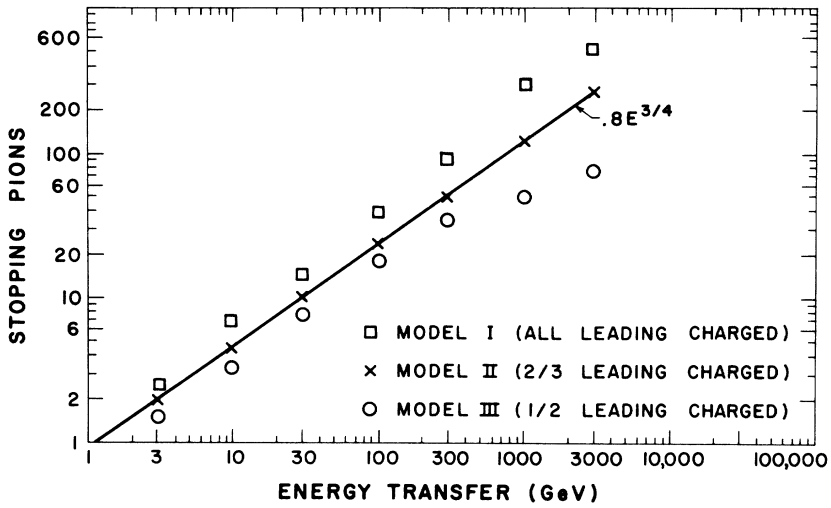

FIG. 1. Multiplicity of stopping pions (sum of π^+ and π^-) in photonuclear-induced hadronic cascades, as a function of the energy E_γ of the initiating photon. For the case of the photonuclear interactions of a muon, E_γ is the energy transfer, ν. The multiplicities used in this paper correspond to Model II of JJT (for which approximately $\frac{2}{3}$ of the leading particles are charged) but the extreme leading-particle assumptions of Model I (all charged) and Model III ($\frac{1}{2}$ charged) are also shown.

The number of interactions with energy transfer ν produced in a target of effective thickness Δx and area Δa normal to a muon beam of energy E and differential intensity $J(E, h, \theta)dE$ is

$$J(E, h, \theta)dE\Delta a \frac{N}{A}\Delta x \frac{d\sigma}{d\nu},$$

where $d\sigma/d\nu$ is the muon inelastic scattering cross section. The number of stopping pions eventually resulting from these interactions is obtained by multiplying by the cascade multiplicity $m(\nu)$ obtained from Sec. III, and the number of pions per g is obtained by dividing by the target mass $\Delta x\Delta a$. Appealing to the equilibrium argument, we may now write for the number of muons stopping per g,

$$q_\mu(h) = \eta \int J(E, h, \theta) \frac{N}{A} \frac{d\sigma}{d\nu} m(\nu) d\nu dE d\Omega, \qquad (7)$$

where N is Avogadro's number, A is the atomic weight of the target material, and η is the fraction of slow pions which decay. The integration is carried out over all incident muon angles and energies, and with limits on ν as discussed below.

B. The Local Muon Spectrum

The local spectrum is easily obtained from the muon intensity-depth curve by differentiation. Let $I(h+x, \theta)$ be the integral muon intensity in the direction θ at distance x beyond a detector at slant depth h underground. Then

$$J(E, h, \theta) = \frac{dI}{dx}(h+x, \theta) \Big/ \frac{dE}{dx} \qquad (8)$$

is the muon spectrum at depth h differential in local energy E. Clearly, x is simply the additional range of a muon (whose energy is E) beyond the detector and dE/dx is its rate of energy loss. It is convenient to introduce the normalized spectrum

$$j(E, h, \theta) = J(E, h, \theta)/I(h, \theta). \qquad (9)$$

To a very good approximation (within 5% at shallow depths and 1% at great depths) $j(E, h, \theta) = j(E, h)$; that is, the normalized spectrum depends only upon slant depth regardless of zenith angle. A series of plots are shown in Fig. 2 in order to illustrate the depth dependence of $j(E, h)$. We estimate the overall accuracy of $j(E, h)$ to be about 10% for energies less than 1000 GeV, the uncertainty coming from uncertainties in the vertical intensity-depth curve. At muon energies above 1000 GeV, straggling becomes important, and consequently, we somewhat overestimate the local spectrum. However, less than 25% of the stopping muon intensity from inelastic scattering comes from muons with energies >1000 GeV, so we have made no attempt to correct for the effects of straggling.

C. Inelastic Muon Scattering Cross Section

We take for $d\sigma/d\nu$ the following expression

$$\frac{d\sigma}{d\nu} = \int_{t\,\mathrm{min}}^{t\,\mathrm{max}} \frac{d^2\sigma(\nu, t)}{d\nu dt} dt, \qquad (10)$$

where $t = |q^2|$, the 4-momentum transfer squared and

$$\frac{d^2\sigma}{d\nu dt} = \Gamma(t, \nu)\left(1 - \frac{t}{m_\rho^2}\right)^{-1} \sigma_\gamma(K) A^{f(K)}. \qquad (11)$$

Here, $\sigma_\gamma(K)$ is the real total photoproduction cross section; $K = \nu - 2M$, the momentum of the virtual photon in the c.m. system of the final-state hadrons; and M and m_ρ are the nucleon and ρ-meson masses, respectively. $\Gamma(t, \nu)$ is the flux of virtual photons associated with the muon given by

$$\Gamma(t, \nu) = \frac{\alpha}{2\pi t}\left(\frac{\nu - t/2M}{p^2}\right)\left(1 - \frac{2\mu^2}{t} + \frac{2E(E-\nu) - \frac{1}{2}t}{\nu^2 + t}\right), \qquad (12)$$

where E, p, and μ are the lab energy, momentum, and mass of the muon, respectively. We have made the following fits for $f(K)$ and $\sigma_\gamma(K)$ to the data of DESY, Santa Barbara-SLAC, and NINA[17] in the regions listed below:

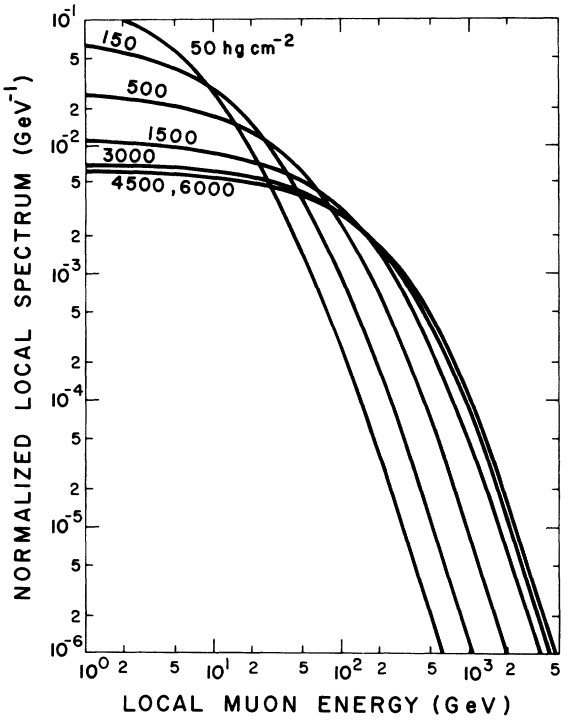

FIG. 2. Normalized local muon spectrum. The spectrum is differential in local muon energy and the areas under the curves are normalized to the vertical muon intensity at each underground depth shown.

(a) Resonance region ($K \leq 1.15$ GeV),

$$\sigma_\gamma(K) = \left[\frac{1.25 m_\pi^2}{[(K-0.32)^2 + \frac{1}{4}m_\pi^2]} + \frac{2.40 m_\pi^2}{[(K-0.7)^2 + \frac{1}{4}m_\pi^2]} + \frac{4.30 m_\pi^2}{[(K-1.0)^2 + 2.25 m_\pi^2]}\right]\sigma_\gamma , \quad (13)$$

$$f(K) = 1.0 ; \quad (14)$$

(b) nonresonance region ($K > 1.15$ GeV),

$$\sigma_\gamma(K) = \sigma_\gamma + 64.9/K^{1/2} , \quad (15)$$

$$f(K) = 0.20 \exp[(1.15 - K)/37.5] + 0.8 . \quad (16)$$

In each region, $\sigma_\gamma = 98.7$ μb. The above fits agree with the data for $K < 20$ GeV. The exponent of A tends toward 0.8 at large K; we have taken this limiting situation since it is currently believed that in a high-energy γ-A collision, the surface nucleons will not completely shield the interior nucleons from possible interaction. Complete shielding, as exhibited in the vector-dominance model, would predict a cross section varying as $A^{2/3}$ at large K. Finally the following limits of integration[18] have been used:

$$\begin{aligned} &\text{(i)}\ \ \nu_{\min} = m_\pi, \text{ the pion rest mass}, \\ &\text{(ii)}\ \ \nu_{\max} = E[1 - (M/2E)(1 + \mu^2/M^2)], \\ &\text{(iii)}\ \ t_{\min} = \mu^2\nu^2/E(E-\nu), \\ &\text{(iv)}\ \ t_{\max} = 2M\nu . \end{aligned} \quad (17)$$

Extrapolations of the real total photoproduction cross section (and particularly its A dependence) to photon momenta greater than 20 GeV are estimated to cause uncertainties in $q_\mu(h)$ of no more than about 50%.

The results of the calculation will be presented in Sec. VI. The ratio of stopping muons from photonuclear interactions to the omnidirectional through-going muon flux is obtained from $R_\mu = Mq_\mu/\bar{A}I_\nu\Omega^* = \bar{t}q_\mu/I_\nu\Omega^*$, where $\bar{t} = M/\bar{A}$ is the effective detector thickness (taken as 100 g/cm^2 unless otherwise stated) and $I_\nu\Omega^*$ is as given in Sec. II. Note that the same muon intensity-depth curve enters in both the numerator and denominator of R_μ, which is sensitive only to the slope of the curve from which is derived the normalized local spectrum.

V. LOCAL MUON PRODUCTION BY REAL PHOTONS

In the electromagnetic case the problem is somewhat complicated since a two step mechanism is involved, namely the initiation of an electromagnetic shower by muon knock-on, bremsstrahlung, or pair production followed by a low-energy hadronic cascade initiated by the photons in the electromagnetic shower. We ignore electroproduction, which is depressed by a factor α. Simplicity is achieved if we again use the equilibrium argument of Sec. IV A. Let $\varphi(E, E_0, x)$ be the probability per unit length that a muon of energy E at distance x from a detector will make an electromagnetic shower of energy E_0. Clearly, φ $(=\varphi_k + \varphi_\gamma + \varphi_p)$ is the sum of the probabilities for the above three processes, and for interactions within a few shower lengths of the detector, the probabilities are independent of x. Let $\pi_\gamma(E_0, \nu, u)$ be the number of photons of energy ν at depth u from the shower origin where the shower energy is E_0. Then, the number of pions generated in a target whose thickness is dt by a muon of energy E is

$$\begin{aligned} n_\pi(E) &= \int_0^R \int_{E_0} \varphi(E, E_0, x)dx \int_x^{x+dt} \int_\nu \pi_\gamma(E_0, \nu, u)\frac{N}{A}\sigma_\gamma(\nu)A^{f(\nu)}m(\nu)d\nu du \\ &= \int_{E_0} \varphi(E, E_0) \int_\nu \frac{N}{A}\sigma_\gamma(\nu)A^{f(\nu)}m(\nu) \int_0^R dx \int_x^{x+dt} \pi_\gamma(E_0, \nu, u)du d\nu \\ &= \int_{E_0} \varphi(E, E_0) \int_\nu \frac{N}{A}\sigma_\gamma(\nu)A^{f(\nu)}m(\nu) \int_0^R dx\, \pi_\gamma(E_0, \nu, x)dt d\nu \\ &= \left[\frac{N}{A}\int_{E_0} \varphi(E, E_0) \int_\nu g(E_0, \nu)\sigma_\gamma(\nu)A^{f(\nu)}m(\nu)d\nu\right]dt , \end{aligned} \quad (18)$$

where R is the range of an electromagnetic shower of energy E_0 and $g(E_0, \nu) = \int_0^R \pi_\gamma(E_0, \nu, x)dx = \int_0^\infty \pi_\gamma(E_0, \nu, x)dx$ is the track length of all the photons in the showers. Thus, folding in the local muon spectrum, we obtain for the local muon source strength due to electromagnetic interactions

$$q_\gamma(h) = \eta \int_E \int_\Omega I(h, \theta)j(E, h, \theta)n_\pi(E)dE d\Omega . \quad (19)$$

The probability of muon knock-on, $\varphi_k(E, E_0)$, has been taken from Rossi,[19] the bremsstrahlung, $\varphi_\gamma(E, E_0)$, has been taken from Petrukhin[20] and Rozental,[21] and the pair production probability, $\varphi_p(E, E_0)$, has been taken from Kokoulin and Petrukhin.[22] Comparisons of the results obtained by using all of Rossi's probabilities with the above showed no significant differences. For the track length, we have used Rossi's approximation A.

For this case, $g(E_0, \nu) = 0.572(E_0/\nu^2)X_0$, where X_0 is the radiation length of rock (30 g cm^{-2}). We have compared these values with those obtained from numerical integrals of the shower distributions given in the Messel tables[23] and have found agreement to within 20%.

The results of the calculation of q_γ will be presented in Sec. VI. R_γ is obtained from q_γ in the manner indicated in Sec. IV for R_μ.

VI. SUMMARY AND COMPARISON WITH EXPERIMENT

A. Summary of Calculations

The results of the preceding sections for the various underground stopping muon components are summarized in Figs. 3–5. Figure 3 gives the rate of stopping positive pions only, at relatively shallow depths, for comparison with experiments which yield this quantity directly. Figure 4 gives the results for all the sources of stopping muons, expressed in the form of the ratio R of stopping to through-going particles. Figure 5 gives the absolute intensity of stopping muons as a function of depth, together with curves for the vertical muon intensity and the omnidirectional muon intensity, $I_V \Omega^*$. Figure 6 gives both the normalized stopping rate and interaction rate as a function of energy transfer. These latter curves allow one to estimate the energies involved in either the observed stopping rate or muon interaction rate underground.

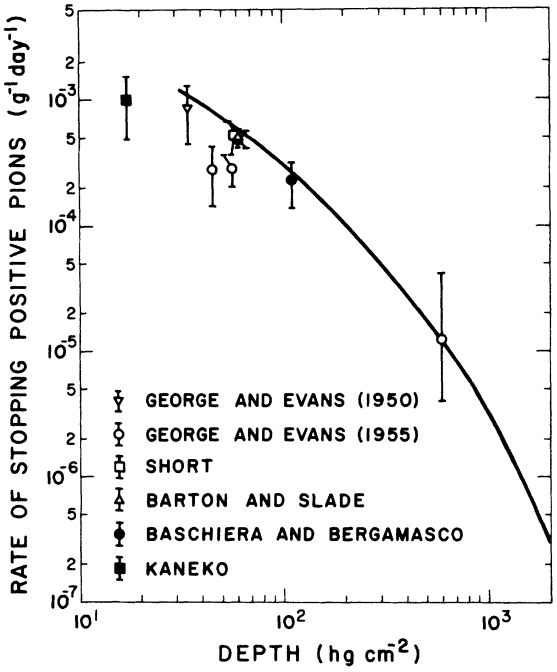

FIG. 3. Calculated rate of stopping *positive* pions vs depth, compared with the results of experiments where the π^+ is identified as such. The solid line gives the sum of the locally produced intensities, $q_\mu(h)$ and $q_\gamma(h)$, with $\eta = 0.5$, as is appropriate for positive pions only. Note that the units are g^{-1} day^{-1}. The experimental results have been corrected after Grupen *et al.*[5] for the loss of π^+ in flight and for the relative stopping power of the different detectors compared to rock.

B. Comments on Calculations

The curves in Fig. 4 have several features which are worthy of comment. For depths less than ~2000 hg cm^{-2}, the atmospheric muon contribution

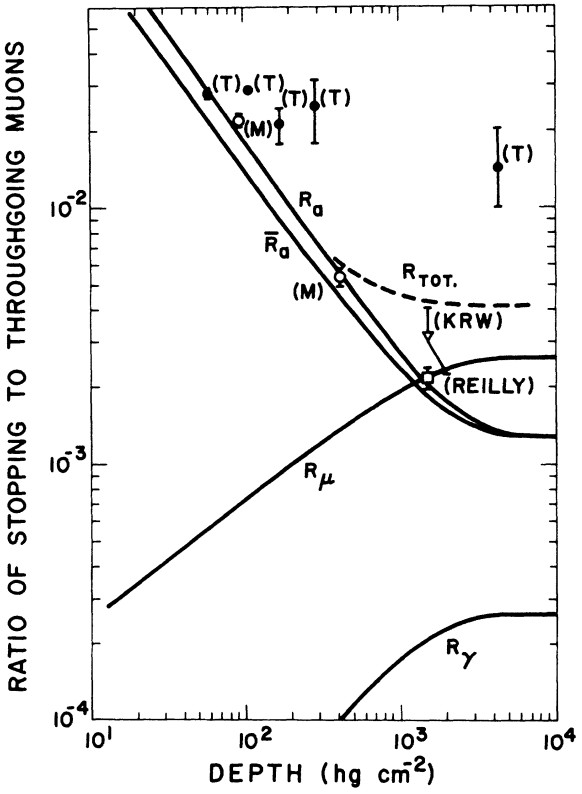

FIG. 4. Normalized rate of stopping muons (ratio R of stopping muons to through-going muons for a standard spherical detector with an effective thickness of 100 g/cm^2 of standard rock, $A = 22$, $Z = 11$). R_a refers to vertical atmospheric muons, $\bar{R}_a$ refers to atmospheric muons integrated over all zenith angles under a flat earth; R_μ, R_γ refer to the ratio of locally produced stopping muons produced by virtual and real photons, respectively, relative to the rate of atmospheric through-going muons integrated over all zenith angles. R_{tot} is the total for all processes. The atmospheric curves (R_a or $\bar{R}_a$) used for comparison with experiment depend upon the experimental triggering disposition.

R_a is inversely proportional to depth while the local production contribution, $R_\mu + R_\gamma$, increases linearly with depth. At depths greater than 3000 hg cm^{-2}, all ratios become depth-independent. This is a reflection of the nature of the muon intensity-depth curve, which is shaped mainly by the power law spectrum of the primaries and the exponential form of the rate of energy loss of muons underground. Moreover, the normalized local muon spectrum (being proportional to the derivative of the intensity-depth curve) should have an increasing fraction of high-energy muons with increasing depth until ~3000 hg cm^{-2}, after which normalized spectrum should become depth-independent. Consequently, the local production ratios should increase with depth up to ~3000 hg cm^{-2}, at which point these ratios, too, would approach a constant. The magnitude of these local production ratios, of course, depends upon the values of cross sections and cascade multiplicities.

C. Comparisons with Stopping Pion Measurements

Measurements of pion stopping rates are available only at relatively shallow depths. We have plotted these measurements[24-29] in Fig. 3, where they may be compared with our calculated curve for stopping positive pions. (Negative pions are not detected in scintillator experiments, and in the emulsion experiments the positive pions are separately identified.) We have also corrected the measurements (after Grupen *et al.*[5]) for the stopping power ratio of the detector material relative to standard rock and the losses by decay in flight of the pions before they reach the detector.

It is seen that the experiments are in reasonable agreement with the calculations. In addition to indicating that there is no anomalous pion production at these depths (<100 hg/cm^2) within the experimental and calculational errors, the agreement provides some confirmation of the validity of our calculations. Of course, the mean muon energy is so low (10–30 GeV) at these depths that the calculations are tested only in the region of low-energy transfers and low cascade energies. However, it is just in the low-energy region that an experimental test of the stopping pion cascade multiplicity is most desirable, as pointed out in Sec. III.

The interactions of muons at shallow depths (50 hg/cm^2) have been studied by Higashi *et al.*[30] using a cloud chamber. Our calculations have not yet been put in a form suitable for detailed comparison with these results. However, the cross section found by these authors (again at a relatively low mean muon energy) appears to be consistent with what we would expect.

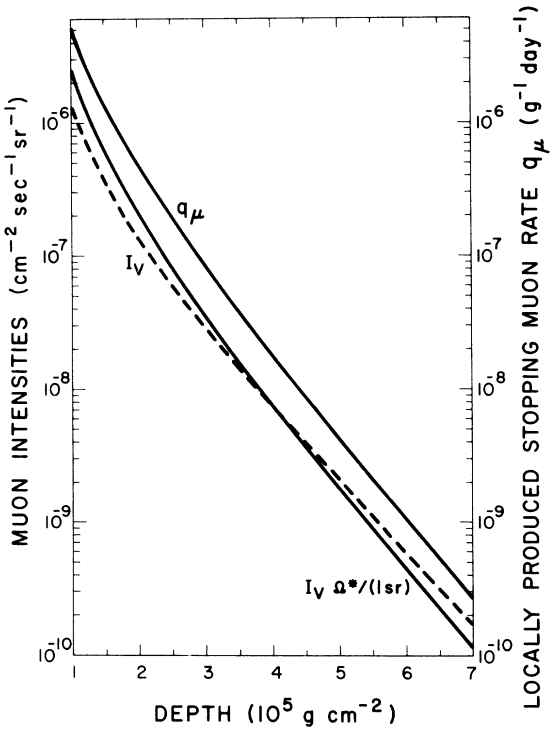

FIG. 5. Absolute integral values of I_V (the vertical muon intensity), $I_V\Omega^*$ (the muon intensity integrated over all zenith angles under a flat earth), and q_μ (the muon stopping rate due to local interactions only) as a function of depth underground. I_V and $I_V\Omega^*$ are read from the left. ($I_V\Omega^*$ has been divided by 1 sr to make the I_V and $I_V\Omega^*$ curves dimensionally the same.) The q_μ curve is read from the right. Muons from interactions initiated by both real and virtual photons associated with the fast muons are included in q_μ, and the parameter η has been taken as 0.7.

D. Comparions with Stopping Muons at Shallow Depths

Inspection of Fig. 4 shows that at depths less than about 2000 hg/cm^2 all measurements are in agreement[1-3,9,26,31,32] with calculations, with the exception of the 3 points of the Turin group at 110, 175, and 300 hg/cm^2. We wish to call attention to the fact that these 3 points were derived from measurements made at various inclined zenith angles at the same station, whose vertical depth was 60 hg/cm^2. Details are given in the paper by Bergamasco *et al.*[3] The trigger for the four shallow Turin measurements included a narrow 2-scintillator telescope without absorber. This arrangement is appropriate to study *atmospheric* muons which arrive at inclined angles and stop in the detector; the ratio R of stopping muons so selected to the inclined through muons should be in agreement with the expectation calculated on the basis of vertical muons at a depth corresponding to the slant

depth in question. However, the response of this arrangement to locally produced muons may differ substantially from what would be expected in a detector located at a vertical depth corresponding to the given slant depth. The locally produced muons are caused essentially by the vertical muon flux, and they are expected to be quasi-isotropic in contrast to the atmospheric muons, whose distribution is peaked toward the vertical. In addition, an open narrow-angle telescope would easily be activated by shower particles associated with the local interaction.

We estimate the ratio R'_μ of locally produced muons to through-going muons actually registered by the Turin inclined-angle disposition as follows. We read from Fig. 5 the rate of local stopping muons, $q_\mu(60\ \text{hg/cm}^2)$. The fraction of these muons accepted by the telescope, of solid angle $\Delta\Omega$, is $\Delta\Omega/4\pi$, and if, in addition, a fraction f of them are accompanied by shower particles which trigger the telescope, we have

$$R' = \frac{Mq_\mu(60)(\Delta\Omega/4\pi + f)}{I(\theta)\Delta\Omega} .$$

From Bergamasco *et al.*[3] we obtain values of $\Delta\Omega$ and $I(\theta)$. For example at 78° (slant depth 300 hg/cm^2), $\Delta\Omega = 0.018$ sr and one finds that a shower triggering probability $f = 2\%$ is sufficient to account for the anomalous excess at this point. According to Fig. 6, some 2% of locally produced stopping muons are produced in events with energy transfers >100 GeV, so that such a value of f is not at all unreasonable. It is somewhat more difficult to account fully for the 110 and 175 hg/cm^2 points, but a strong effect undoubtedly exists.

A further enhancement in steeply inclined measurements is due to the multiple scattering of slow muons, originally coming in from the vertical, which scatter and register as inclined muons. A correction ranging from 5% at 60° to 75% at 78° has been estimated for this effect by Grupen *et al.*[5] These authors, however, apply their correction to the observed point as though it consisted entirely of stopping atmospheric muons, when in fact a more appropriate procedure, in the light of the foregoing, would be to raise the prediction for the atmospheric muon component only by this amount.

The experiment of Bhat and Ramana Murthy[9] at 96 hg/cm^2 and 417 hg/cm^2 was also performed with a large volume liquid scintillator. A liquid scintillation counter was located above the primary detector with 2.5 cm of lead in between. The aperture was relatively large (zenith angles $\lesssim 20°$). Consequently, we would expect their apparatus to be sensitive primarily to atmospheric stopping muons (which are dominant at that depth) and, indeed, their point falls close by the prediction in Fig. 4. It should be noted, however, that the through muon rate was not measured in their experiment, so their quoted values for R depend on a normalization to the through flux, and this can lead to additional uncertainty.

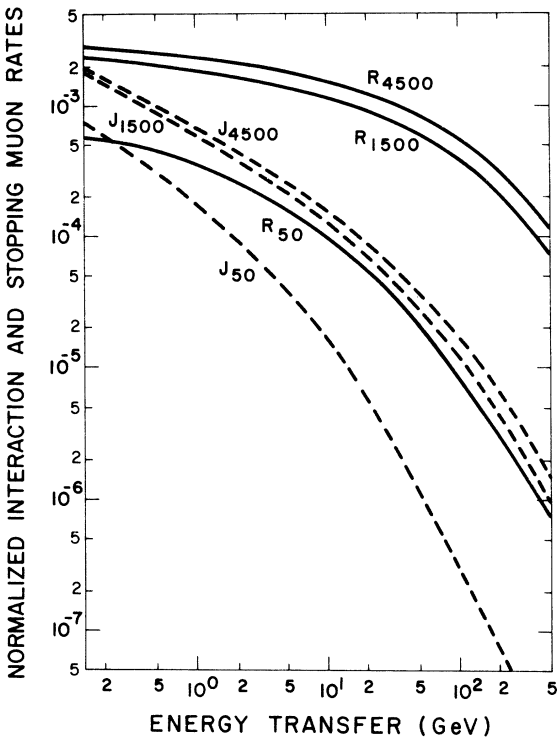

FIG. 6. Integral muon interaction and stopping rates (due to local interactions only) as a function of energy transfer. The curves are normalized to the rate of muons passing through a standard detector whose effective thickness is 100 g/cm^2 of standard rock ($A = 22$, $Z = 11$). The curves labeled J are the interaction rates; the curves labeled R are the stopping rates. The subscripts refer to depth underground in hg cm^{-2}. The R-curves may be used in the following way: at 4500 hg cm^{-2} approximately 10% of the observed stopping muons due to local interactions originated from interactions with greater than 200-GeV energy transfer.

The experiment by Kropp, Reines, and Woods,[31] performed at a depth of 1568 hg/cm^2 also employed a large volume of liquid scintillator. There was no directional selection; however, the detector was surrounded by a large volume of water and a thick iron shield. We estimate $\eta \sim 0.5$ for this case rather than 0.7 as for an open cavity. The dense shield also means that the interactions producing pions would occur near the detector, in some cases saturating the electronics and making the scope picture unreadable. This measurement should lie somewhat below our total prediction, and indeed it does.

The detector of Reilly *et al.*[32] was triggered only if a system of auxiliary counters on the top and sides showed one and only one pulse, and a bottom counter observed no pulse. The auxiliary counters were very large (1.5 m×2.5 m) and the thresholds low, making it likely that stopping particles produced by the interaction of a fast muon would be vetoed by the fast muon or shower activity accompanying it. Thus, we would expect the Reilly *et al.* point to lie somewhat above the atmospheric prediction and somewhat below the prediction for atmospheric plus local effects. This is seen to be the case in Fig. 4, although statistically the results are not in disagreement with the total prediction.

E. Comparison with the Deep Turin Point

The most important point from the standpoint of observing possible anomalies is the Turin point at 4270 hg/cm^2. At this depth the atmospheric muon contribution is well below the conventional local production contribution. For this measurement a 500-liter spherical liquid scintillator was used without a directional telescope in the trigger. The results therefore correspond directly to our calculation with only a correction for the effective thickness of the scintillator (69 g/cm^2 of standard rock, as compared with our 100 g/cm^2).

We give in Table I our expectations for this particular scintillator. Included also in Table I are the probabilities for the Turin observation to have occurred for our preferred and extreme models. There is only one chance in twenty that the Turin measurement agrees with our calculations. Since about 90% of the local stopping rate comes from energy transfers less than 100 GeV (see Fig. 6), there seems to be little room for large increases beyond our upper limit within the conventional framework.

F. Comparison with Other Calculations

Our results are in reasonable agreement with those of Baschiera *et al.*[2] and Grupen *et al.*,[5] although we feel that the latter did not sufficiently stress the uniqueness of the deep Turin point. We disagree with Barton[6] mainly because he assumed that the stopping pion multiplicity increased linearly with the mean local muon energy, starting at shallow depths. Our calculations would give an increase more like the $\frac{3}{4}$ power. Adair's[4] estimate disagrees with ours because his rough estimate of the stopping pion multiplicity is higher than ours.

G. A Comment on Neutrino-Induced Stopping Muons

As pointed out especially by Grupen *et al.*,[5] at very great depths (~8000 hg/cm^2) the predicted stopping-muon rate is predominantly from neutrino interactions, and the observations of Reines *et al.*[33] are in reasonable agreement with prediction. It is difficult to draw any conclusions about the existence of an anomalous underground process at these depths in view of our lack of knowledge of the depth dependence of such a process and the uncertainty of how the neutrino detectors would respond to the (possibly very complex) events involved. It would be interesting to investigate further the isolated cases of very large events which have been seen in the deep neutrino detectors and which appear to have no ready explanation at present.

VII. CONCLUSIONS

We conclude that at shallow depths, where the mean muon energy is in the 10-GeV region and where the atmospheric stopping muon component is dominant, no stopping muon measurements are inconsistent with the calculations of this paper. The stopping pion observations (available only at shal-

TABLE I. Values of the predicted and observed stopping-muon ratios for the Turin 4270-hg cm^{-2} experiment. The upper bound prediction reflects an $A^{1.0}$ dependency of the photonuclear cross section (instead of $A^{0.8}$) as well as a slow muon multiplicity predicted from Model I, as outlined in Sec. III. Only the calculations of R_μ are affected, a factor of 1.6 coming from the photonuclear cross section and 1.5 from the multiplicity. Any further increases would involve radical alterations in the photonuclear cross section. The R values quoted refer to the Turin detector (effective thickness 69 g/cm^2 of rock).

Stopping-muon ratio	Prediction		Observation
	Best estimate	Upper bound	
R_a	0.88×10^{-3}	0.88×10^{-3}	
R_μ	1.77×10^{-3}	4.23×10^{-3}	
R_γ	0.18×10^{-3}	0.18×10^{-3}	
R_{TOT}	2.8×10^{-3}	5.3×10^{-3}	$9.8^{+4.0}_{-3.0}\times10^{-3}$
Number actual events	3	6	11
Probability of observing ≥ 11	0.003	0.03	

low depths) are also in agreement with our calculations.

The Turin measurement at 4270 hg/cm^2 is uniquely sensitive to a possible anomalous source of stopping muons, and here we have seen that there is a considerable excess relative to our predictions. We have examined the A dependence of the photonuclear cross section and various models for hadronic cascades without being able to account for the discrepancy under even the most extreme assumptions.

Some confirmation of the low-energy end of our hadronic cascade calculations does come from the consistency of our predictions with stopping pion rates observed (Fig. 3). A direct measurement of $m(\nu)$ in the accelerator range is important to check the calculation. Knowledge of the number of stopping pions produced in a γ-initiated hadronic cascade, even at a few low energies, would strengthen our knowledge of $m(\nu)$ for all energies, because of the multiplicative nature of the cascade processes.

Needless to say, it is very important to obtain additional Turin-type observations beyond, say, 3000 hg/cm^2, and/or with improved visual identification of the events. Such measurements are in progress in this laboratory.

---

*Research supported by the National Science Foundation.

†Present address: Department of Physics, University of Pittsburgh, Pittsburgh, Pa., 15213.

[1]B. Baschiera, L. Bergamasco, C. Castagnoli, and P. Picchi, Lett. Nuovo Cimento 4, 121 (1970).

[2]B. Baschiera, L. Bergamasco, C. Castagnoli, and P. Picchi, Lett. Nuovo Cimento 1, 961 (1971).

[3]L. Bergamasco, C. Castagnoli, M. C. Tabasso, and P. Picchi, Accademia Nazionali dei Lincei 48, 423 (1970).

[4]R. K. Adair, Lett. Nuovo Cimento 2, 891 (1971).

[5]C. Grupen, A. W. Wolfendale, and E. C. M. Young, Nuovo Cimento 10B, 144 (1972).

[6]J. C. Barton, in Proceedings of the Twelfth International Conference on Cosmic Rays, Hobart, Tasmania, 1971 (unpublished).

[7]J. W. Keuffel, Lett. Nuovo Cimento 2, 669 (1971).

[8]For example, for the Turin detector, density 0.88 g/cm^3, stopping power relative to standard rock 1.2, the effective thickness is $\frac{4}{3}$(0.88 g/cm^3)(49 cm) (1.2) =6.9 g/cm^2, so all results are to be multiplied by $\frac{100}{69}$.

[9]P. N. Bhat and P. V. Ramana Murthy, in Proceedings of the Twelfth International Conference on Cosmic Rays, Hobart, Tasmania, 1971 (unpublished).

[10]C. T. Stockel, Ph.D. thesis, University of London (unpublished).

[11]S. Miyake, J. Phys. Soc. Japan 18, 1093 (1963).

[12]D. E. Groom, Univ. of Utah Internal Note No. UUCR 102 (unpublished).

[13]P. H. Barrett, L. M. Bollinger, G. Cocconi, Y. Eisenberg, and K. Greisen, Rev. Mod. Phys. 24, 133 (1952).

[14]J. L. Morrison, Univ. of Utah Internal Note No. UUCR 106-107, 1970 (unpublished).

[14]H. E. Bergeson, G. L. Bolingbroke, G. W. Carlson, D. E. Groom, J. W. Keuffel, J. L. Morrison, and J. L. Osborne, Phys. Rev. Letters 27, 160 (1971).

[16]W. V. Jones, D. P. Johnson, and J. A. Thompson, preceding paper, Phys. Rev. D 7, 2013 (1973).

[17]G. Wolf, in *Proceedings of the 1971 International Symposium on Electron and Photon Interactions at High Energies, 1971,* edited by N. B. Mistry (Cornell Univ. Press, Ithaca, N. Y., 1971), p. 170; M. L. Perl, T. Braunstein, J. Cox, F. Martin, W. T. Toner, B. D. Dieterle, T. F. Zipf, W. L. Lakin, and H. C. Bryant, Phys. Rev. Letters 23, 1191 (1969).

[18]G. L. Cassiday, Phys. Rev. D 3, 1109 (1971).

[19]B. Rossi, *High Energy Particles* (Prentice-Hall, Englewood Cliffs, N. J., 1952), p. 16.

[20]A. A. Petrukhin and V. V. Shestakov, Can. J. Phys. 46, S377 (1968).

[21]I. L. Rozental, Usp. Fiz. Nauk 94, 91 (1968) [Sov. Phys. Usp. 11, 49 (1968)].

[22]R. P. Kokoulin and A. A. Petrukhin, in Proceedings of the Twelfth International Conference on Cosmic Rays, Hobart, Tasmania, 1971 (unpublished).

[23]H. Messel and D. F. Crawford, *Electron-Photon Shower Distribution Function Tables* (Pergamon, New York, 1970).

[24]A. M. Short, Proc. Phys. Soc. (London) 81, 841 (1963).

[25]L. Bergamasco, Nuovo Cimento 66B, 120 (1970).

[26]J. C. Barton and M. Slade, in *Proceedings of the Ninth International Conference on Cosmic Rays* (Institute of Physics and the Physical Society, London, 1965), p. 1006.

[27]E. P. George and J. Evans, Proc. Phys. Soc. (London) A63, 1248 (1950).

[28]E. P. George and J. Evans, Proc. Phys. Soc. (London) A68, 829 (1955).

[29]S. Kaneko, T. Kubozoe, M. Okazaki, and M. Takahata, J. Phys. Soc. Japan 10, 600 (1955).

[30]S. Higashi, T. Kitamura, Y. Mishima, S. Miyamoto, Y. Watase, and H. Shibata, Nuovo Cimento 38, 107 (1965).

[31]W. R. Kropp, F. Reines, and R. M. Woods, Phys. Rev. Letters 20, 1451 (1968).

[32]T. Reilly, Ph.D. thesis, Case Western Reserve University, 1970 (unpublished).

[33]F. Reines, W. R. Kropp, H. W. Sobel, H. S. Gurr, and J. Lathrop, Phys. Rev. D 4, 80 (1971).